Supporting Information

Yoon et al. 10.1073/pnas.1004153107

SI Materials and Methods

Expression and Purification of MD-1. MD-1 was expressed in insect cells by a baculovirus expression system. MD-1 encoding cDNA (residues 21–160 for cMD-1 and residues 20–162 for mMD-1) was amplified by PCR and ligated into a modified pAcGP67 baculovirus transfer vector (BD Biosciences) that contains C-terminal, thrombin cleavage site and His_6 tag. Recombinant baculovirus was obtained by transfecting SF9 insect cells with the cloned plasmid DNA and linearized baculovirus DNA (AB vector). MD-1 protein was expressed for 2 d after infecting Hi-5 insect cells with amplified recombinant virus. Secreted protein was purified by Ni-NTA affinity chromatography and Mono Q anion exchange chromatography. After thrombin digestion, the resulting protein was purified by gel filtration chromatography. MD-$1^{\text{lipid IVa}}$ was obtained by mixing purified MD-1 protein and synthesized lipid IVa (Peptide International) in a molar ratio of 1:2, and purified from unbound components by a Mono Q column.

MD-1/LPS Interaction Analysis. To analyze the MD-1/LPS interaction, native PAGE and gel filtration were used. *Escherichia coli* LPS or its variant LPS Ra (Sigma-Aldrich and List Biological Laboratories) was solubilized by sonication either in water or buffer [20 mM Hepes (pH 7.4), 150 mM NaCl] and incubated with MD-1 for 2–3 h at room temperature. To examine competition of MD-1 with polymyxin B for LPS, MD-1 was incubated with polymyxin B for 2 h before LPS was added. The MD-1/LPS or MD-1/LPS/polymyxin B mixture was loaded onto a native gel, and electrophoresis was performed in running buffer [25 mM Tris, 190 mM glycine (pH 8.8)]. The interaction was also confirmed by gel filtration on a Superdex 200 HR 10/30 column in running buffer [20 mM Hepes (pH 7.4), 150 mM NaCl, 1 mM EDTA].

Crystallization and Data Collection. cMD-1^{PGT} and cMD-$1^{\text{lipid IVa}}$ were crystallized at 23 °C by sitting-drop, vapor diffusion. cMD-1^{PGT} crystals were obtained by mixing 0.5 μL of protein solution (11 mg/mL) with 0.5 μL of well solution containing 18% PEG 4000 and 100 mM Hepes (pH 7.0). cMD-$1^{\text{lipid IVa}}$ crystals were generated by mixing 0.5 μL of cMD-1/lipid IVa solution (10 mg/mL) with 0.5 μL of well solution containing 17% PEG 2000 and 100 mM Mes (pH 6.0). cMD-1^{PGT} crystals were derivatized in 10 mM di-μ-iodo-bis-ethylenediamine-diplatinum (II) nitrate (PIP) for experimental phasing. Crystals were cryoprotected by 25% glycerol. Native and PIP derivative X-ray diffraction data of cMD-1^{PGT} were collected at the Stanford Synchrotron Radiation Lightsource (SSRL) beamline 11-1 and at the Advanced Light Source (ALS) beamline 8.2.2., respectively. cMD-$1^{\text{lipid IVa}}$ diffraction data were collected at the Advance Photon Source (APS) beamline 23ID-B. X-ray data were processed with *HKL2000* (1). Data collection statistics are summarized in Tables S1 and S2.

Structure Determination and Refinement. The cMD-1^{PGT} structure was determined by SIRAS phasing (Table S1). Heavy-atom sites were located by *SHELXD* (2), and phases were calculated by *MLPHARE* (3). The resulting phases were density modified by *DM* (4). The initial model was manually built in the density-modified, electron density map using the hMD-2 structure (PDB ID code 2e56) as a template. The cMD-1^{PGT} structure was iteratively built using *COOT* (5) and refined with *REFMAC5* (6). The cMD-$1^{\text{lipid IVa}}$ structure was solved by molecular replacement with *PHASER* (7) using the refined cMD-1^{PGT} structure as a search model. The final cMD-$1^{\text{lipid IVa}}$ structure was obtained by iterative model building and refinement. Refinement statistics are summarized in Table S2.

1. Otwinowski Z, Minor W (1997) Processing x-ray diffraction data collected in oscillation mode. *Methods Enzymol* 276:307–326.
2. Sheldrick GM (2008) A short history of SHELX. *Acta Crystallogr A* 64:112–122.
3. Collaborative Computational Project, Number 4 (1994) The CCP4 suite: Programs for protein crystallography. *Acta Crystallogr D* 50:760–763.
4. Cowtan K (1994) 'dm': An automated procedure for phase improvement by density modification. *Joint CCP4 ESF-EACBM Newslett Protein Crystallogr* 31:34–38.
5. Emsley P, Cowtan K (2004) Coot: Model-building tools for molecular graphics. *Acta Crystallogr D Biol Crystallogr* 60:2126–2132.
6. Murshudov GN, Vagin AA, Dodson EJ (1997) Refinement of macromolecular structures by the maximum-likelihood method. *Acta Crystallogr D Biol Crystallogr* 53:240–255.
7. McCoy AJ, et al. (2007) Phaser crystallographic software. *J Appl Cryst* 40:658–674.

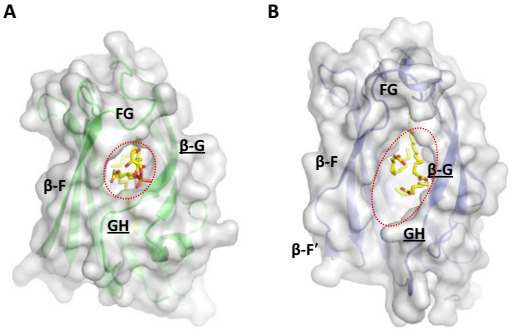

Fig. S1. cMD-1 (*A*) and hMD-2 (*B*; PDB ID code 2e56) shown with a transparent surface over ribbons. The cavity entrance is highlighted with red broken lines. Molecules found in the hydrophobic cavity are represented by sticks (carbon, yellow; oxygen, red; phosphorus, orange). A PGT molecule was built in the cMD-1 structure compared with three myristoyl acid molecules that were built into the hMD-2 structure.

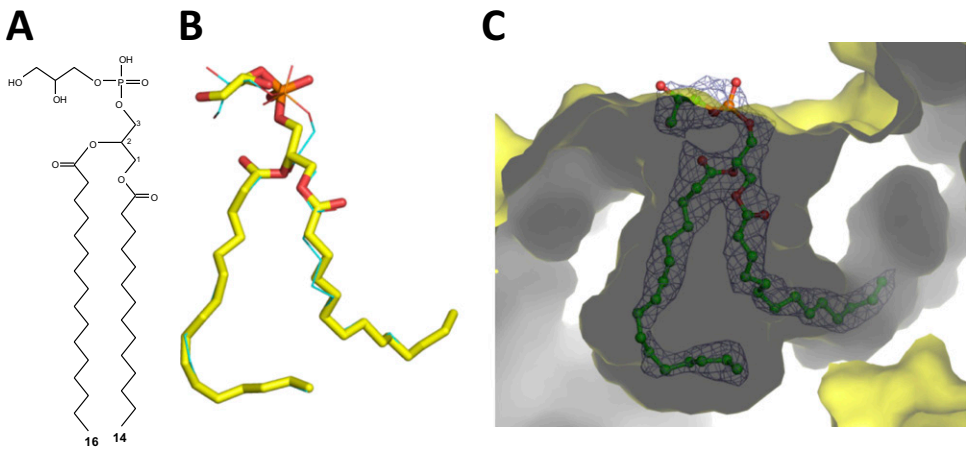

Fig. S2. A putative PGT molecule in the cMD-1 structure and its corresponding electron density. (*A*) Schematic representation for PGT. (*B*) Comparison of the two PGT molecules in the asymmetric unit. (*C*) A PGT molecule (a ball-and-stick model) with its electron density (0.7 σ in $2F_o–F_c$ map) inside the cMD-1 cavity (yellow/gray surface).

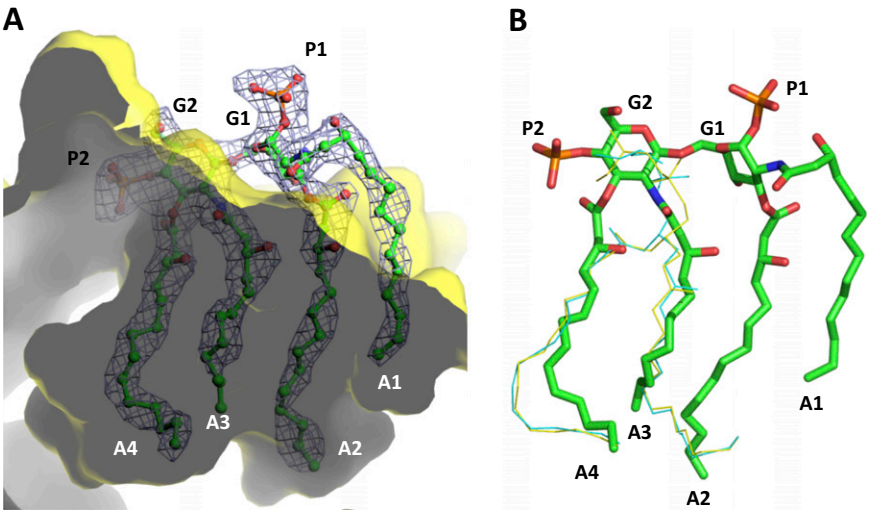

Fig. S3. Lipid IVa bound to cMD-1. (*A*) A lipid IVa molecule (a ball-and-stick model) with its electron density (1.0 σ in $2F_o–F_c$ map) inside the cMD-1 cavity (yellow/gray surface). (*B*) Comparison of lipid IVa (green) and PGT (cyan and yellow).

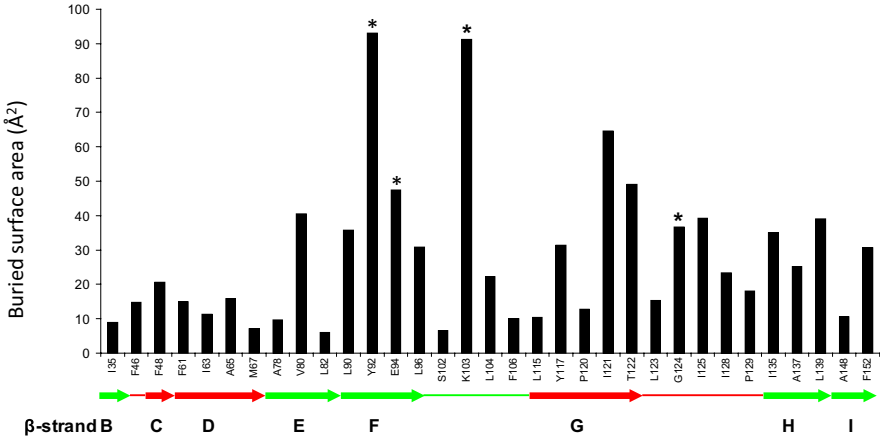

Fig. S4. cMD-1 accessible surface area buried by lipid IVa in the cMD-1/lipid IVa structure. MD-1 secondary structure is represented by thick arrows for β-strands and thin lines for loops, and is colored in green for the sheet-1 side and in red for the sheet-2 side. cMD-1 residues that form H bonds with lipid IVa are designated with stars above the buried surface area bars.

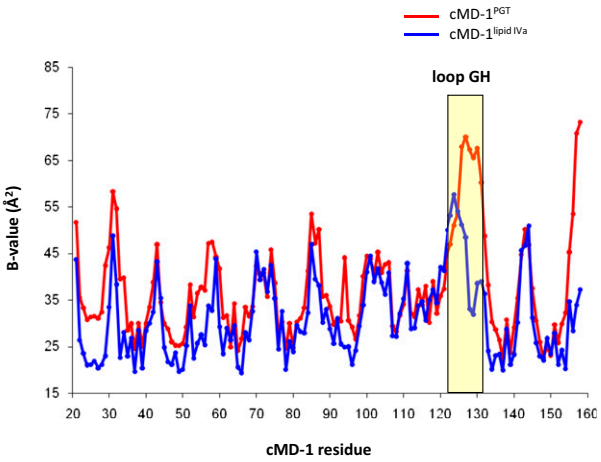

Fig. S5. Average B-values for each residue in structures of cMD-1^{PGT} (red) and cMD-1$^{lipid\ IVa}$ (blue). Loop GH is boxed in yellow.

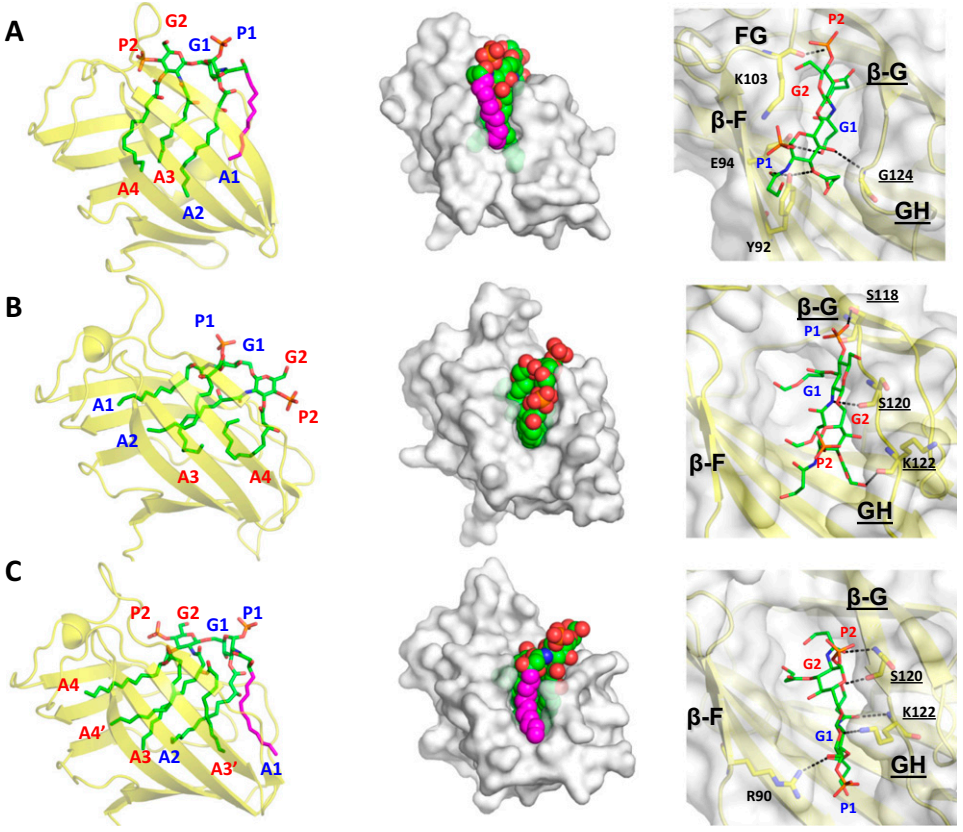

Fig. S6. Comparison of lipid IVa$_{cMD-1}$ (*A*), lipid IVa$_{hMD-2}$ (*B*; PDB ID code 2e59), and LPS$_{hMD-2/hsTLR4}$ (*C*; PDB ID code 3fxi) structures. The molecule orientation of each column is identical to that of Fig. 6. MD-1 and MD-2 are presented by ribbon diagram (yellow) or surface representation (gray). The ligand is shown in sticks or spheres (carbon, green; oxygen, red; nitrogen, blue; phosphorus, orange). Exposed acyl chain A1 is highlighted in magenta. (*Right*) Only hydrophilic portion of ligand is shown for clarity, and H bonds are represented by dashed lines.

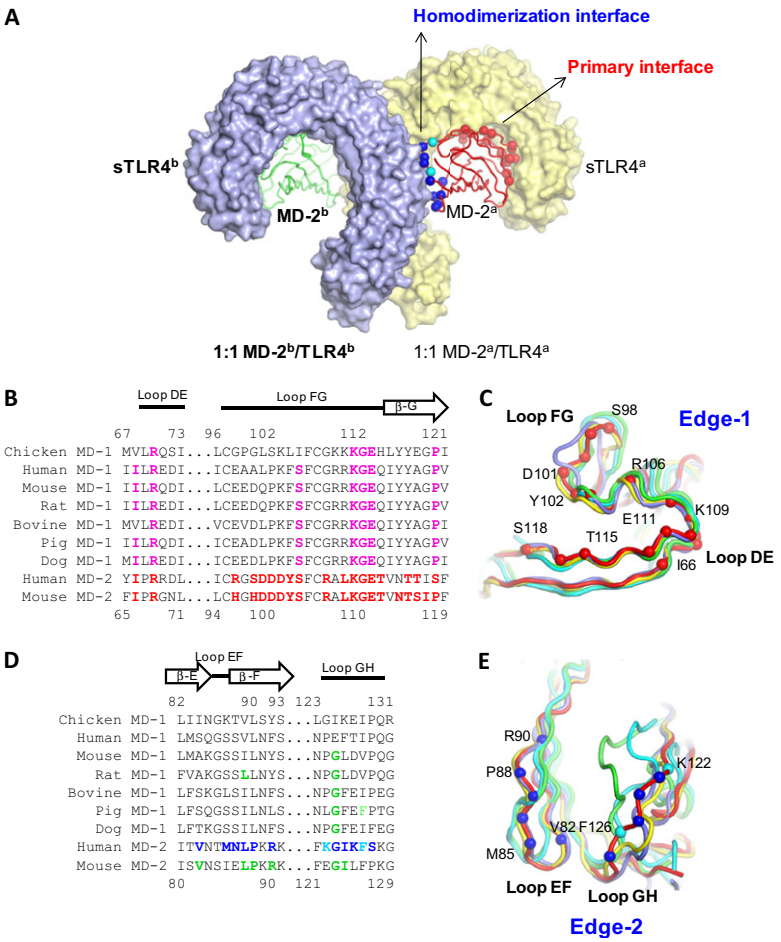

Fig. S7. Comparison of MD-1 and MD-2 in the primary and homodimerization interfaces. (*A*) LPS-bound hMD-2/hsTLR4 structure (PDB ID code 3fxi). MD-2 and sTLR4 are shown in coils (MD-2^{a}, red; MD-2^{b}, green) and surface representations (sTLR4^{a}, yellow; sTLR4^{b}, light blue), respectively. In the absence of an agonist ligand, such as LPS, MD-2 and sTLR4 form a heterodimeric complex (MD-2^{a}/sTLR4^{a} or MD-2^{b}/sTLR4^{b}) using the primary interface (red spheres). LPS binding induces homodimerization of the 1:1 MD-2/sTLR4 complex, and as a result, a homodimerization interface (blue spheres) is formed between two 1:1 complexes. hMD-2 residues 122 and 126 are also shown in spheres (cyan). (*B*) MD-1 and MD-2 sequence alignment in the primary interface. MD-2 residues observed in the primary interface are colored in red. MD-1 residues conserved with the MD-2 interface residues are colored in magenta. (*C*) Structural comparison of MD-1 and MD-2 in the primary interface. Five structures are overlaid and shown in coils: cMD-1^{PGT} (green); cMD-1$^{lipid\ IVa}$ (cyan); hMD-2 (light blue; PDB ID code 2e56); mMD-2 (yellow) bound to msTLR4 (mMD-2^{msTLR4}; PDB ID code 2z64); hMD-2 (red) bound to hsTLR4/LPS (hMD-2$^{hsTLR4/LPS}$; PDB ID code 3fxi). hMD-2$^{hsTLR4/LPS}$ residues in the interface are represented by red spheres. (*D*) MD-1 and MD-2 sequence alignment in the homodimerization interface. hMD-2 residues are colored according to the color scheme of *A*. MD-1 and mMD-2 residues conserved with the hMD-2 residues are colored in green. (*E*) Structural comparison of cMD-1^{PGT} (green), cMD-1$^{lipid\ IVa}$ (cyan), hMD-2 (light blue), mMD-2^{msTLR4} (yellow), and hMD-2$^{hsTLR4/LPS}$ (red) in the homodimerization interface. hMD-2$^{hsTLR4/LPS}$ residues in the homodimerization interface are represented by blue spheres. Additionally, hMD-2$^{hsTLR4/LPS}$ residues 122 and 126 are shown in cyan spheres.

Table S1. Data collection and phasing statistics for crystallographic data used to determine the cMD-1^{PGT} structure by SIRAS phasing

	PIP derivative	Native
Data collection		
Space group	$P2_12_12_1$	$P2_12_12_1$
Cell parameters, Å	a = 40.21	a = 39.90
	b = 77.06	b = 76.84
	c = 102.37	c = 102.38
Wavelength, Å	1.0720	0.9794
Resolution, Å	30.00–2.40	50.00–2.20
Highest resolution, Å	2.49–2.40	2.28–2.20
No. observations	74,821	143,981
No. unique reflections	12,440	16,458
R_{merge} (%)*	7.2 (28.2)†	9.0 (48.9)†
I/sigma	30.7 (3.8)†	34.0 (5.2)†
Completeness (%)	97.0 (81.9)†	99.9 (99.8)†
Redundancy	6.0 (3.8)†	8.7 (8.2)†
Phasing		
Resolution, Å	15.00–3.00	
No. Pt (SHELXD)	6	
Acentric phasing power	1.11	
Centric phasing power	0.87	

*$R_{merge} = \sum_{hkl}\sum_i|I_i(hkl) - <I(hkl)>|/\sum_{hkl}\sum_i I_i(hkl)$.
†Numbers in parentheses were calculated from data of the highest-resolution shell.

Table S2. Crystallographic statistics of the cMD-1^{PGT} and cMD-1$^{lipid\ IVa}$ structures

	cMD-1^{PGT}	cMD-1$^{lipid\ IVa}$
Data collection		
Space group	$P2_12_12_1$	$P2_12_12_1$
Cell parameters, Å	a = 40.12	a = 39.47
	b = 76.49	b = 78.15
	c = 101.94	c = 101.24
Wavelength, Å	0.9795	1.0333
Resolution, Å	30.00–2.00	20.00–2.40
Highest resolution, Å	2.07–2.00	2.49–2.40
No. observations	147,581	53,788
No. unique reflections	21,878	12,503
R_{merge} (%)*	7.7 (49.7)†	9.1 (37.1)†
I/sigma	36.1 (4.7)†	28.0 (6.6)†
Completeness (%)	99.4 (97.3)†	98.2 (97.6)†
Redundancy	6.8 (5.8)†	4.4 (4.3)†
Refinement		
Resolution, Å	30–2.00	20–2.40
No. of reflections, total	20,652	11,843
No. of reflections, test	1,095	612
R_{cryst} (%)‡	22.1	23.2
R_{free} (%)¶	25.2	26.7
Average B value, Å^2	37.0	32.1
No. protein atoms	2,153	2,181
No. water molecules	146	95
No. ligand atoms	94 (PGT)	186 (lipid IVa)
	6 (glycerol)	18 (glycerol)
	10 (triethylene glycol)	
Rmsd bonds, Å	0.017	0.017
Rmsd angles, °	1.72	1.69
Ramachandran,§ favored	96.7%	96.4%
Ramachandran,§ outliers	0.0%	0.4%

*$R_{merge} = \sum_{hkl}\sum_i|I_i(hkl) - <I(hkl)>|/\sum_{hkl}\sum_i I_i(hkl)$.
†Numbers in parentheses were calculated from data of the highest-resolution shell.
‡$R_{cryst} = \Sigma|\ |F_{obs}|-|F_{calc}|\ |/\Sigma|F_{obs}|$ where F_{calc} and F_{obs} are the calculated and observed structure factor amplitudes, respectively.
¶R_{free} = as for R_{cryst}, but for 5% of the total reflections chosen at random and omitted from refinement.
§Calculated using MolProbity (http://molprobity.biochem.duke.edu/).